Microwave-assisted Synthesis of Mixed Ligand Complexes of Zn(II), Cd(II) and Hg(II) Derived from 4-aminopyridine and Nitrite Ion: Spectral, Thermal and Biological Investigations

Karuthakannan Dhaveethu, Thiagarajan Ramachandramoorthy*, and Kandasamy Thirunavukkarasu[†,*]

PG and Research Department of Chemistry, Bishop Heber College (Autonomous), Tiruchirappalli 620 017, India
*E-mail: chemtr@yahoo.co.in
[†]National Centre for Catalysis Research (NCCR), Indian Institute of Technology Madras, Chennai 600 036, India.
*E-mail: kthirunavukkarasu@gmail.com
(Received March 11, 2013; Accepted May 8, 2013)

ABSTRACT. Zn(II), Cd(II) and Hg(II) complexes with a general composition $[M(L)_2(X)_2]$, where L=4-aminopyridine (4AP) and X=NO_2^- were prepared under microwave irradiation. The metal complexes were characterized by elemental analyses, molar conductance, IR, Far-IR, electronic, NMR (^1H, ^{13}C), XPS spectral and thermal studies. The spectroscopic studies reveal the composition, different modes of bonding, electronic transition, different chemical environment of C and H atoms and the electronic state of the metal atoms. On the basis of the characterization data, tetrahedral geometry is suggested for all the complexes. The free ligand (4-aminopyridine) and their metal complexes were screened against phytopathogenic fungi and bacteria in vitro and the activities were compared.

Key words: Mixed ligand complexes, 4-aminopyridine, Nitrito, Biological activities

INTRODUCTION

It is well documented that heterocyclic compounds of N-donor ligand systems play a significant role in many biological systems being a component of several vitamins and drugs.[1,2] Particularly 4-aminopyridine (4AP) is a potassium channel blocker and it is widely used in pharmacological and medical applications.[3–5] 4AP generally acts as a monodentate, Lewis base ligand through nitrogen of the pyridine ring. The 4AP complexes are used as asymmetric catalysts for various reactions like hydrogenation, cyclopropanation, epoxidation.[6] Metal complexes of 4AP show more effective biological activities than free ligands and free metal ions.[7] According to Tweedy's theory of chelation, chelation reduces the polarity of the metal ions which in turn increases the lipophilic nature of the complexes and it favors the permeability of the complexes through the lipid layers of the microorganisms.[8–10] The nitrite ion (NO_2^-) can coordinate to a metal ion in nine different coordination modes[11] and the metal nitrito complexes may act as photochemical nitric oxide precursors.[12] There are many literature reports available in the past decade on the synthesis, characterization and microbial activities of metal complexes with a complicated ligands derived from 4AP.[13–15] But no report is available on a simple 4AP ligand – metal complex and its biological activity to the best of our knowledge.

Microwaves are nowadays used in chemical reactions as they interact directly with the reactants and hence drive the chemical reactions more effectively.[16–18] Moreover, the use of microwave irradiation has more advantages than the conventional methods because of the following reasons:[19–20] 1) reduction of reaction time from many hours to few minutes, 2) its instantaneous 'in-core' heating of materials in a homogeneous and selective manner, 3) its ability to increase the probability of molecular impacts, 4) decrease in the activation energy and 5) no need of solvents.

The present work aims at the microwave-assisted synthesis and spectral characterization of $M[(L)_2(X)_2]$ complexes, where M = Zn(II), Cd(II) and Hg(II) ions, L = 4-aminopyridine (4AP) and X = NO_2^- ions along with the investigation of their thermal behavior by TGA and DTA. The complexes were screened for antibacterial and antifungal activities and the results were discussed.

EXPERIMENTAL

All the chemicals used were of AR grade from Sigma-Aldrich and were used as received. Ethanol was distilled over calcium oxide before use. Microwave irradiations were used for the synthesis of complexes from domestic microwave oven (model IFB-25 PG 1S) at 900W power for 10 seconds.
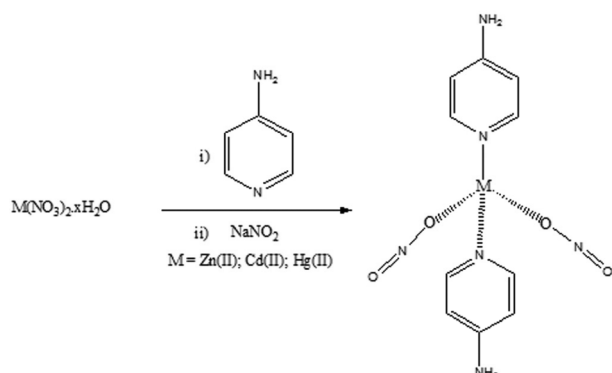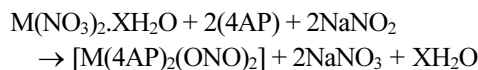
Figure **1.** Preparation of metal complexes.

Synthesis of the Complexes

A warm ethanolic solution (20 ml) of zinc nitrate hexahydrate $Zn(NO_3)_2.6H_2O$ (0.58 g, 2 mmol)/cadmium nitrate tetrahydrate, $Cd(NO_3)_2.4H_2O$ (0.42 g, 2 mmol/mercuric nitrate monohydrate, $Hg(NO_3)_2.H_2O$ (0.70 g, 2 mmol) were mixed together with warm ethanolic solution (20 ml) of 4AP (0.38 g, 4 mmol) with constant stirring. The resulting solution was then treated with an ethanolic suspensions of sodium nitrite (0.26 g, 4 mmol) with continuous stirring. After keeping the mother liquor for few hours, the corresponding complexes of Zn(II) (**1**), Cd(II) (**2**) and Hg(II) (**3**) (*Fig.* 1) were filtered, washed with cold ethanol and dried in a vacuum desiccator over anhydrous calcium chloride.

$$M(NO_3)_2.XH_2O + 2(4AP) + 2NaNO_2$$
$$\rightarrow [M(4AP)_2(ONO)_2] + 2NaNO_3 + XH_2O$$

Where, M = Zn(II), Cd(II) and Hg(II); 4AP = 4-aminopyridine.

Physical Measurements

Elemental analyses (carbon, hydrogen and nitrogen) were carried out using Elementar Vario EL III (Germany) model analyzer. The metal content was estimated by volumetric and Atomic Absorption Spectrometry. Molar conductances were measured in DMF on the Equiptronics, digital conductivity meter, (Model EQ-660), where the cell constant was calibrated with 0.1 M KCl solution and DMF was used as the solvent. The IR Spectra (4000–400 cm^{-1}) were taken at 27 ºC using Perkin Elmer spectrometer, model Spectrum X1 in KBr disc and Far-IR spectra were taken at 27 ºC using FT-IR Thermo Nicolet (model 6700) spectrometer in which polyethylene was used as calibrant. The electronic spectra were recorded by the diffused reflectance technique on Varian Cary (model 5000) Spectrophotometer. The ^{1}H NMR and ^{13}C NMR spectra of the organic ligand and the complexes were recorded in d6- DMSO on a BRUKER 500 MHz spectrometer at room temperature using TMS as an internal reference.

Cyclic voltammograms of the complexes at concentration 10^{-3} M in the solution of Tetra Butyl Ammonium Bromide (TBABr) – DMF were recorded at room temperature. Redox potentials were recorded in Ag/AgCl reference electrode and glassy carbon as working electrode, at the scan rate 100 mVs^{-1}. The thermal analyses were carried out using universal V4.5A Thermal Analyzer Instruments (SDT Q 600 V20.5 Build 15). The XPS measurements were carried out using a multiprobe system (Omicron Nanotechnology, Germany) equipped with a dual Mg/Al X-ray source and a hemispherical analyzer operating in constant analyzer energy (CAE) mode. The spectra were obtained with pass energy of 50 eV for survey scan and 20 eV for individual scans; a Mg Kα X-ray source was operated at 300 W and 15 kV. The base pressure in the analyzing chamber was maintained at 1×10^{-10} mbar. The data were processed with the Casa XPS program (Casa Software Ltd., U.K.). The peak areas were determined by integration employing a Shirley-type background. Peaks were considered to be a mix of Gaussian and Lorentzian functions in a 70/30 ratio. For the quantification of the elements, relative sensitivity factors (RSF) provided by the manufacturer were used. The peaks were calibrated by taking the adventitious carbon's C 1s line as 284.9 eV.

Antimicrobial Screening

Cultures of phytopathogenic bacteria such as *Raoultella planticola* (MTCC, 2272), *Shigella flexineri* (MTCC, 1457) and *Pseudomonas aeruginosa* (MTCC, 1688) and fungi such as *Aspergillus niger* (MTCC, 961) and *Candida albicans* (MTCC, 183) were procured from, Microbial type culture collection and gene bank, Chandigarh, India and maintained on slants of potato dextrose agar (PDA) and nutrient agar (NA) media.

Antibacterial Activity Measurements

Antibacterial activities of the complexes were tested with well diffusion technique.[21] Twenty milliliter of sterilized nutrient agar (NA) media was poured in each pettriplates. After solidification 0.1 ml of test bacteria spreads over the medium using a spreader. The test compounds in measured quantities were dissolved in DMF to get concentrations of 100, 75, 50 and 25 µgml^{-1} (*Fig.* 2). Using sterile cork borer (6 mm in diameter), four holes were made in each dish, then tested compounds dissolved in DMF were poured into these holes. Finally, the dishes were incubated
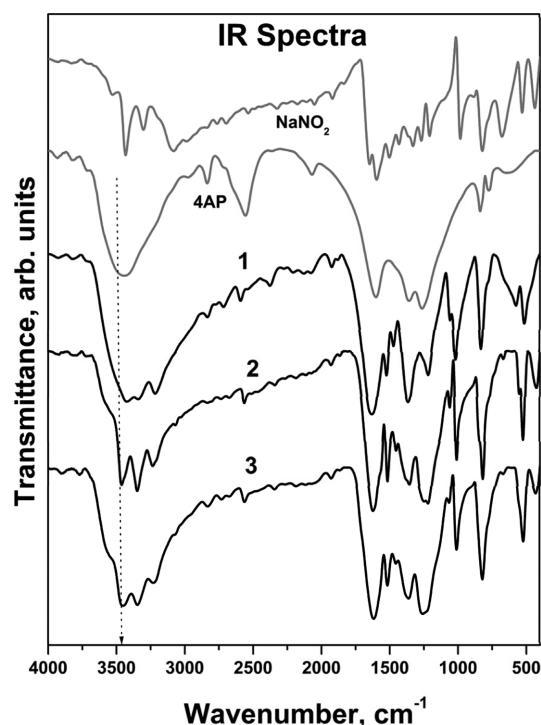
Figure 2. IR Spectra of the ligands alone (4AP and NaNO$_2$) with the complexes **1**, **2** and **3**.

at 37 $^{\circ}$C for 24 hours where clear or inhibition zones detected around each hole. DMF served as control and streptomycin used as a standard drug under the same conditions for each organism and by subtracting the diameter of inhibition zone resulting with DMF from that obtained in each case, the antibacterial activities were calculated as a mean of three replicates.

Antifungal Activity Measurements

Aspergillus niger and Candida albicans fungi were used as the test organism for which the growth inhibition capacity of the ligand (4AP) and its complexes have been screened. According to the agarplate technique[22] the compounds were directly mixed to the DMF in different (400, 200, 100 μgml^{-1}) concentrations. The fungus was placed on the medium with the help of the inoculum needle. The Pettridishes were wrapped in polythene sheets carefully, con-

taining some drops of ethyl alcohol and put in incubater at 30±1 $^{\circ}$C for 48−72 h. Chlorothalonil used as commercial fungicide and DMF served as control. The growth of fungus was measured by the recording the diameter of fungal colony.

RESULTS AND DISCUSSION

On the basis of elemental analyses, the complexes were found to have the composition as shown in *Table* 1. The low molar conductance measurements of the complexes in DMF correspond to their non-electrolyte nature and hence it can be inferred that NO$_2^-$ ligand present in the coordination sphere.[23]

Infrared Spectra

The IR Spectra of the ligands 4AP, nitrite ion and the metal complexes are given in *Fig*. 2. The complexes **1**, **2** and **3** and the free ligand 4AP show bands at 1647, 1596 and 1502 cm^{-1}, typical for the pyridine skeleton[24,25] and the out of plane peak at 822 cm^{-1}. 4AP has two nitrogen atoms and both of them can coordinate to the metal ion. When amino nitrogen atom is involved in coordination a drastic red shift observed in NH$_2$ stretching vibration (Δ = 150−200 cm^{-1}).[24]

Since there is no red shift in NH$_2$ stretching vibrations, amino nitrogen of 4AP does not involve in coordination in the complexes **1**, **2** and **3**. The ring breathing mode observed at 983 cm^{-1} for 4AP, is observed at 1018 cm^{-1}, 1010 cm^{-1} and 1007 cm^{-1} for the complexes **1**, **2** and **3** respectively. This mode is known to be very sensitive to coordination of pyridine from the ring nitrogen atom and the wave number increases with the strength of the coordination bond.[26,27] Thus it is concluded that ring nitrogen is involved in the coordination in the complexes studied.

The nitrite group has three fundamental vibrational modes which are all active in the infrared region and upon coordination, the band positions are shifted as compared to the free nitrite frequencies. The shift exhibited by the asymmetric and symmetric stretching frequencies are used to indicate the mode of bonding of the nitrite group,

Table 1. Elemental analyses and molar conductance of the compounds

Compounds	Colour	Yield %	Analysis found (calcd) %				
			M	C	H	N	∧m (Ω^{-1}cm^2 mol^{-1})
C$_5$H$_6$N$_2$ (4AP)	Colourless	–	–	63.79 (63.83)	6.27 (6.32)	29.74 (29.78)	–
ZnC$_{10}$H$_{12}$N$_6$O$_4$ (**1**)	Pale brown	78	18.98 (18.99)	34.82 (34.87)	3.53 (3.56)	24.38 (24.42)	16.4
CdC$_{10}$H$_{12}$N$_6$O$_4$ (**2**)	White	66	28.72 (28.84)	30.63 (30.68)	3.12 (3.18)	21.52 (21.57)	14.7
HgC$_{10}$H$_{12}$N$_6$O$_4$ (**3**)	Dirty White	65	41.82 (41.86)	24.98 (24.98)	2.54 (2.58)	17.52 (17.56)	21.6

whether it coordinates through nitrogen atom (nitro complex) or through the oxygen atom (nitrito) complex.[28] In the nitrito complexes, $\nu_{as}(NO_2)$ lies at higher and $\nu_s(NO_2)$ at lower values than the free ion frequencies.[29–31] In case of nitro complexes, both $\nu_{as}(NO_2)$ and $\nu_s(NO_2)$ are shifted to higher frequencies as compared to the free nitrite ion.[32,33] The absence of wagging mode (640 cm^{-1}) in the complexes **1**, **2** and **3** is another evidence for the nitrito complexes.[34] The N–O stretching band of the complexes **1**, **2** and **3** appears in the region between 850 and 750 cm^{-1}.[35] The bands in the region of 452–480 cm^{-1} and 510–530 cm^{-1} in the spectra of the complexes are assigned to stretching frequencies of (M–N) and (M–O) bonds respectively.[36] The ν (M–O) of nitrito complexes were assigned in the 360–320 cm^{-1} region[37] and observed for the complexes **1**, **2** and **3** also.

In a recent publication[38] one of our authors have reported the single crystal XRD data of [Cd(4-AAP)$_2$(NO$_2$)$_2$] complex (where, 4-AAP refers 4-aminoantipyrene) with FT-IR results. The ORTEP diagram from single crystal XRD of their complex [Cd(4-AAP)$_2$(NO$_2$)$_2$] reveals the bidentate nature of the nitrito ligand. IR spectrum of the complex in the publication shows 842 cm^{-1} corresponds to deformation mode (δ_w) with the absence of wagging mode corresponds to nitro group. It is worth to not here that symmetric and asymmetric stretching vibrations were not observed for their complex. On the other hand, the complexes **1**, **2** and **3** reported here also shows deformation feature at ~830–820 cm^{-1} (a red shift) along with features at ~1050 cm^{-1} and ~1460 cm^{-1} corresponding to ν_s and ν_{as} respectively. Our results are in good agreement with the reported the δ_w, ν_s and ν_{as} IR bands of Choi et al.[39] for their Cr(III) complex, in which nitrite (ONO) acts as a monodentate ligand. Hence we conclude that the complexes reported here have monodentate nitrito ligands.

Electronic Spectra

The electronic vibration (UV-visible) spectra of the metal complexes are given in *Fig.* 3. As the metal ions involved in the complexes are group 12 elements, their stable +2 oxidation state results in d^{10} configuration. The electronic spectra of complexes **1**, **2** and **3** do not show any band corresponds to the central metal ion and the bands observed are mainly due to the ligands and metal-to-ligand interactions. The diffused reflectance spectra of the complex **1** give band at 248–258 nm is due to $\pi \rightarrow \pi^*$ transition of the aromatic ring of 4AP and the band at 320–375 nm is due to n$\rightarrow \pi^*$ transition of the "–N=O" from the complex.[40] It proves that the nitrite ligand coordinated to the metal ions
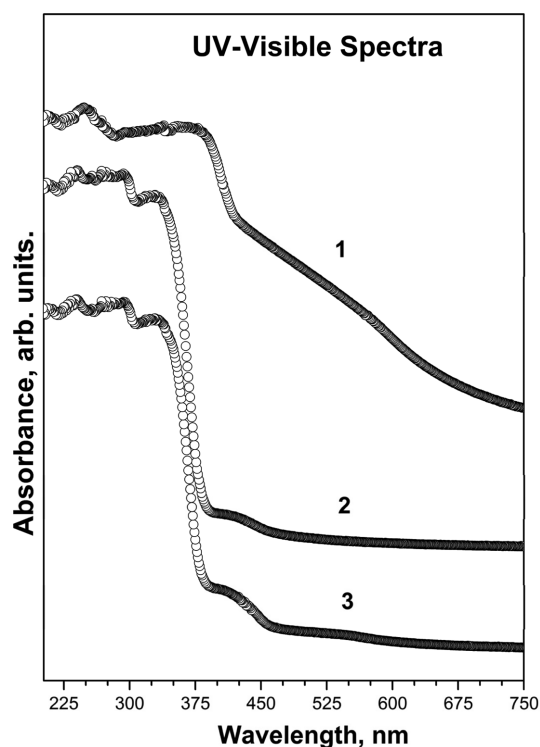

Figure **3.** Electronic Spectra of the complexes **1**, **2** and **3** in the UV-visible region.

in a monodentate fashion as we have seen in the previous section.

In complex **2**, the band at 240–315 nm is due to $\pi \rightarrow \pi^*$ transition of aromatic ring and an intense band at 340–360 nm is due to n$\rightarrow \pi^*$ transition of chromophoric and auxochromic groups. In complex **3**, $\pi \rightarrow \pi^*$ and n$\rightarrow \pi^*$ transitions appear at 250–275 nm and 320–340 nm respectively. The last band below 250 nm in all complexes might be due to L$\rightarrow$M charge transfer band. It has been reported that a metal is capable of forming d-p bands with ligands containing nitrogen as donor atoms.[41]

When group 12 elements are coordinated through N or O donors, the resulting complexes prefer tetrahedral coordination.[42] The analytical data of complexes **1**, **2** and **3** (*Table* 1) also confirm the tetrahedral geometry.

NMR Spectra

The ^{1}H NMR spectra of the complexes **1**, **2** and **3** display three signals, two belonging to aromatic protons and one to amine protons (*Fig.* 4. and *Table* 2). The signals of the amino group protons as well as H-3 proton are found to be shielded in all the complexes. In the ^{13}C NMR spectra of the complexes **1**, **2** and **3**, all the aromatic carbon atoms shifted 0.04–1.33 ppm downfield relatively to the
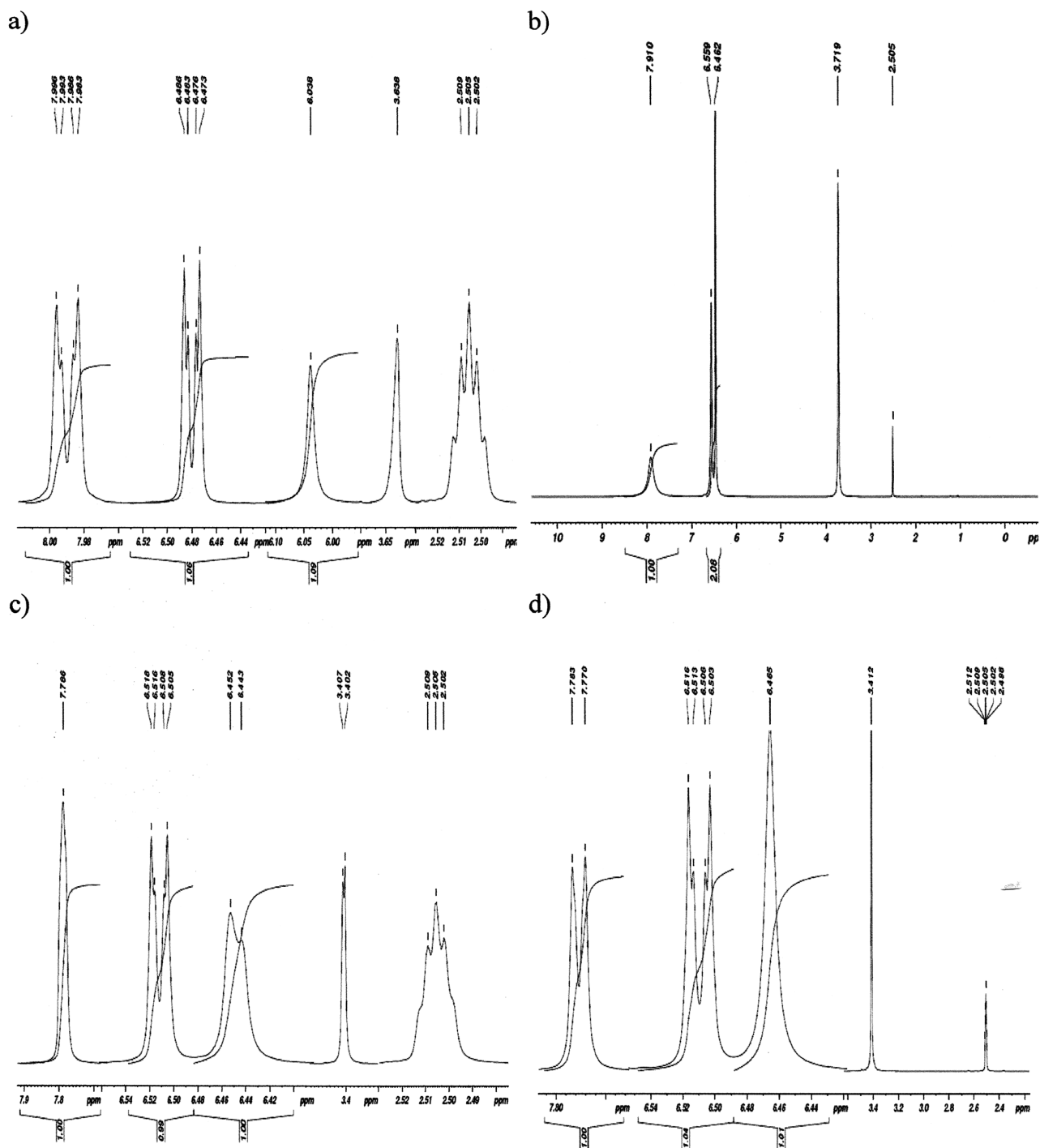
a)

b)

c)

d)

Figure 4. ^{1}H NMR of 4AP (a) and the complexes **1** (b), **2** (c) and **3** (d).

corresponding ones in the parent ligand molecule (C-2, C-3 and C-NH$_2$). These shifts are tabulated in *Tabl*e 3. On the basis of the ^{13}C spectra (*Fig.* 5) it could be concluded that aromaticity of the pyridine ring is preserved upon complexation. Similar conclusions were already made by IR

spectral studies (Section 3.1). The complexation of the complex **1** in C-3 is more pronounced than in complexes **2** and **3**. The amine carbons in **2** and **3** are found to be more shielded than in **1**.

***Table* 2.** ^{1}H NMR chemical shifts (δ ppm^{-1})^a, complexation shifts ($\Delta\delta$ ppm^{-1})^{b,c} and H-H coupling constants (J_{HH}/H$_Z$)^d in the mixed ligand metal complexes

Type of proton		4AP	Complex **1**	Complex **2**	Complex **3**
	δ	7.99	7.91	7.78	7.78
H-2	J_{HH}	7.98(q)	broadened	broadened	7.77(d)
	$\Delta\delta$	–	−0.08	−0.21	−0.21
	δ	6.48	6.55	6.51	6.51
H-3	J_{HH}	6.47(q)	6.51(q)	6.50(q)	6.50(q)
	$\Delta\delta$	−q	0.07	0.03	0.03
	δ	6.04	6.46	6.45	6.46
H-(NH$_2$)	J_{HH}	(s)	broadened(s)	broadened(s)	broadened(s)
	$\Delta\delta$	–	0.42	0.41	0.42

^{a}Referred to TMS in DMSO solutions.
^{b}Complexation shifts are defined as the difference of proton chemical shifts between the complex and parent molecule.
^{c}Sign (+) denotes deshielding effect, while (−) denotes shielding effect.
^{d}Digital resolution ± 0.30 Hz; (s)singlet, (d)doublet, (q)quartet.

***Table* 3.** ^{13}C NMR chemical shifts (δ ppm^{-1})^a and complexation shifts ($\Delta\delta$ ppm^{-1})^{b,c} in the mixed ligand metal complexes

Type of carbon		4AP	Complex **1**	Complex **2**	Complex **3**
C-2	δ	149.98	148.88	149.25	149.21
	$\Delta\delta$	–	−1.1	−0.73	−0.77
C-3	δ	109.40	109.67	109.37	109.35
	$\Delta\delta$	–	0.27	−0.04	−0.05
C-NH$_2$	δ	154.72	155.90	156.03	156.05
	$\Delta\delta$	–	1.18	1.31	1.33

^{a}Referred to TMS in DMSO solutions.
^{b}Complexation shift is defined as the difference of carbon chemical shifts in the complex and the parent molecule.
^{c}Sign (+) denotes deshielding effect, while (−) denotes shielding effect.

Electrochemical Behaviour

The cyclic voltammograms of the complexes **1**, **2** and **3** in 10^{-3} M TBABr (Tetrabutyl ammonium bromide) – DMF^{43} solution were recorded at room temperature using a glassy carbon as working electrode (radius of the micro electrode is 3 mm and the scan rate was 100 mVs^{-1}). The complexes **1** and **2** (*Fig.* 6) exhibit one oxidation and one reduction peaks due to the nature of the nitrito ligand.^{44} But from the CV results, it is clear that the metal ions of complexes **1** and **2** (Zn and Cd) exhibit invariable +2 oxidation state. In complex **3**, there may be existence of one electron couple Hg(II)/Hg(I) at $E_{pa} = 1.46$ V and $E_{pc} = 1.52$ V. This couple found to be quasi-reversible with $\Delta E_p = 0.06$ V and the ratio of anodic to cathodic peak currents corresponding to simple one electron process. The oxidation and reduction peaks of all the three complexes are very little like their oxidation-reduction potential difference (ΔE) because of the nature of coordination of the nitrite ligand, i.e., nitrito. If nitro ligand is present, these peaks would have been well resolved as it can be easily reducible.

Thermal Analyses

The TGA/DTA curves of metal complexes are shown in

Fig. 7. The thermal degradation of the complex **1** consists of three steps. The first step involves a possible elimination of atmospheric moisture from the complex. An exothermic peak is observed at 115.8 ^{o}C due to structural rearrangement of the complex.^{45} The second decomposition step (190–450 ^{o}C) corresponds to the removal of two aminopyridine moieties and two NO groups with mass loss of 58% (calcd. 63.69%). An endothermic peak observed at 326.6 ^{o}C due to the melting process of the complex. The third decomposition step starts at 450 ^{o}C and continues until 1050 ^{o}C corresponding to the loss of metal oxide, (ZnO) residues of about 26% (calcd. 23.56%).

The thermal decomposition of the complex **2** consists of four stages. The first decomposition stage (140–300 ^{o}C) corresponds to the loss of NO$_2$ and NO molecules with the mass loss of 20% (calcd. 19.36%) and this stage contains an exothermic peak at 193.3 ^{o}C. The second decomposition step (300–400 ^{o}C) corresponds to the removal of two NH$_2$ groups with the mass loss of 9% (calcd. 8.15%). The third broad step from 400 to 900 ^{o}C is due to the loss of two pyridine moieties with mass loss of 32.1% (calcd. 40.26%). The sixth decomposition step within the temperature range of 900–1150 ^{o}C corresponds to loss of metal
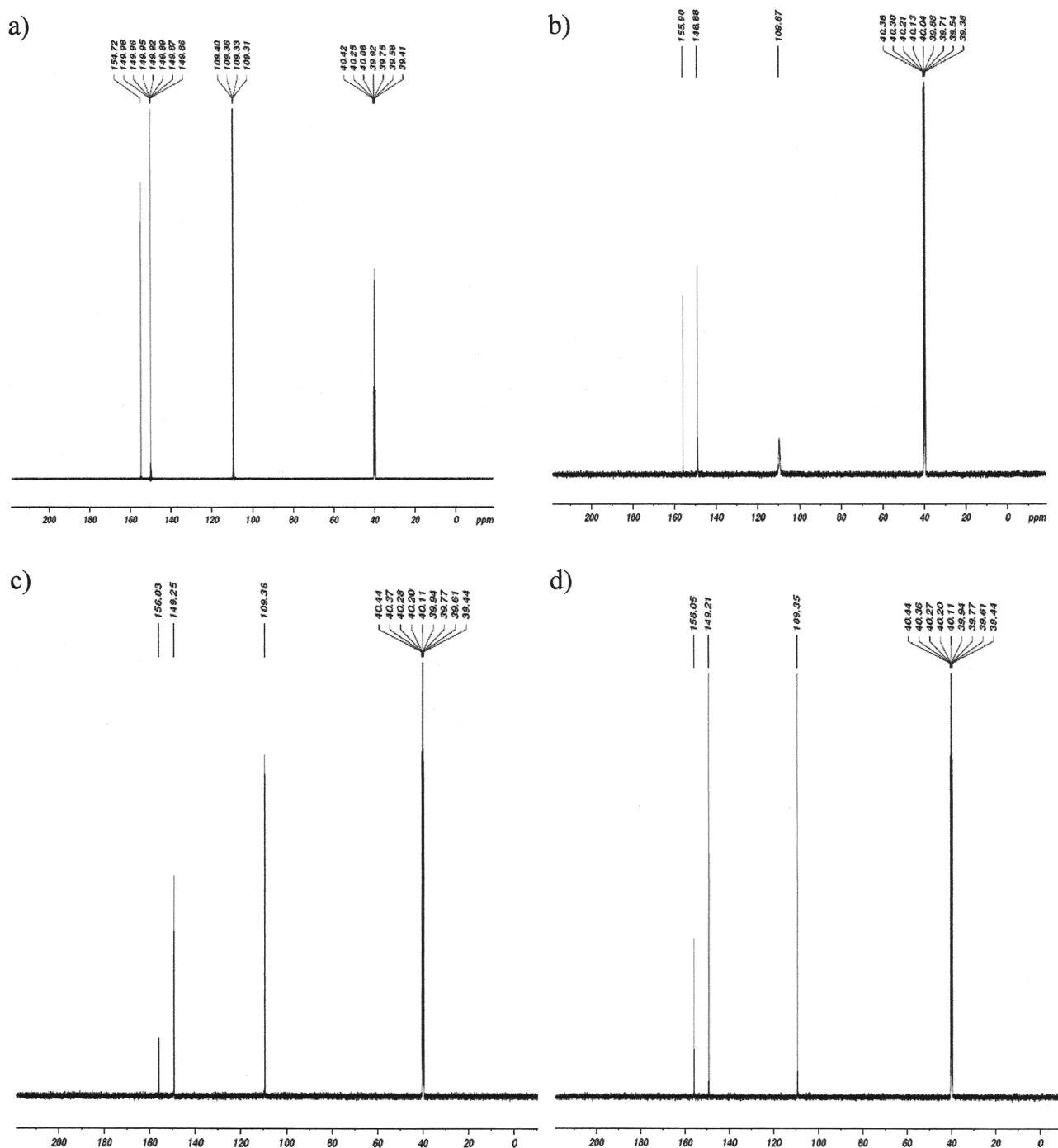
Figure 5. ^{13}C NMR of 4AP (a) and the complexes **1** (b), **2** (c) and **3** (d).

oxide (CdO) as the final residue about 32% (calcd. 28.64%).

The thermal decomposition of the complex **3** also consists of four stages. The first decomposition (150–280 °C) can be attributed to the removal of NO$_2$ and NO group with the mass loss of 22% (calcd. 19.14%). The second decomposition step (280–450 °C) is due to the loss of one

aminopyridine molecule with the mass loss of 20% (calcd. 19.55%). The third step (450–900 °C) corresponding to the elimination of another aminopyridine molecule of mass loss about 20.6% (calcd. 19.55%). The last step starts from 900 °C and continues upto 1200 °C corresponding to the metallic oxide (HgO) residues constituting about 29%
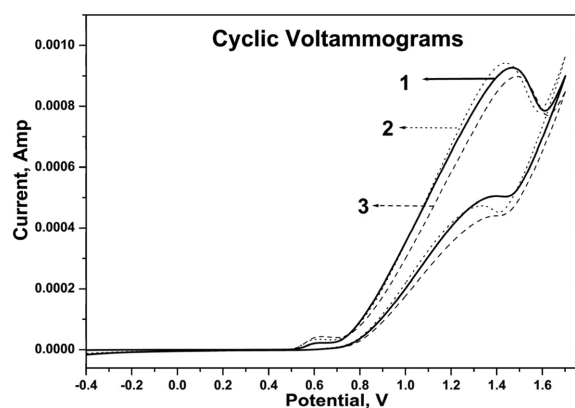
Figure 6. Cyclic voltammograms of **1** (solid line), **2** (dotted line) and **3** (dashed line).
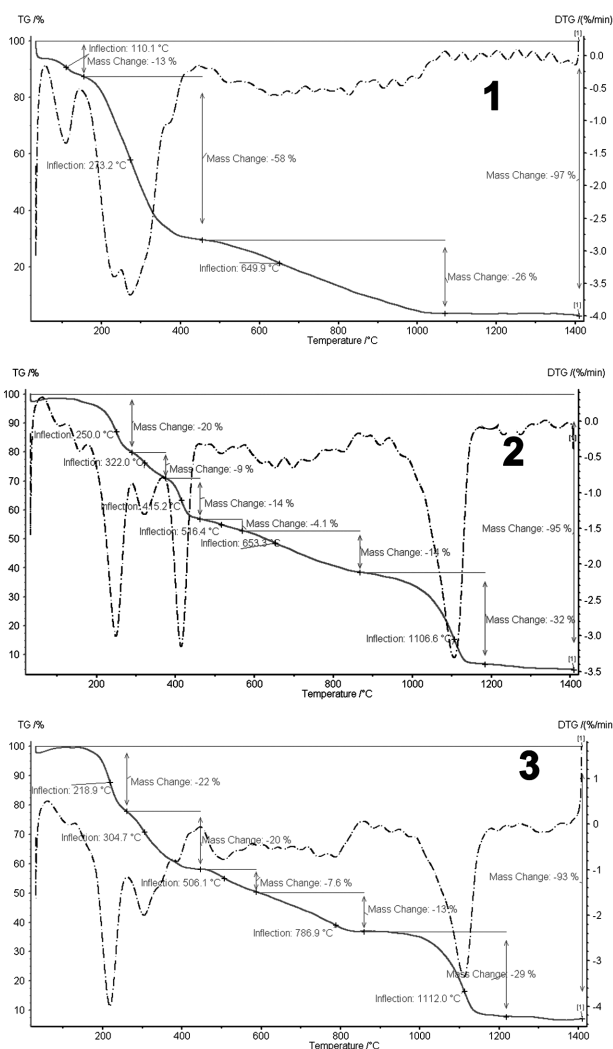

Figure 7. TGA-DTA curves of the complexes **1**, **2** and **3**.

(calcd. 31.6%). These steps are accompanied by exothermic peaks at 159.8 and 520 °C. Thus the complexes may
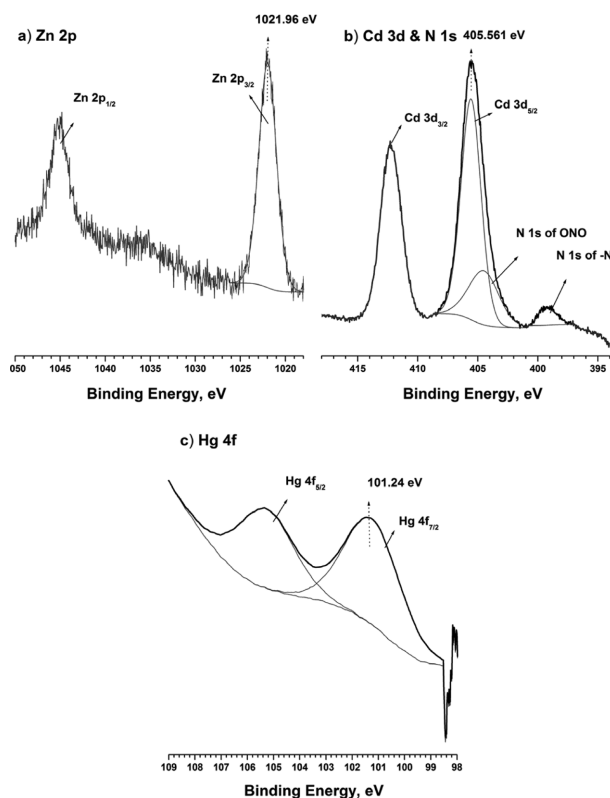

Figure 8. XPS of a) Zn 2p, b) Cd 3d and c) Hg 4f of the complexes **1**, **2** and **3** respectively.

be formulated as $[M(L)_2(X)_2]$, where M=Zn(II), Cd(II) and Hg(II), L=4-aminopyridine; X= NO_2^-.

XPS Studies

Fig. 8 shows the XP spectra of Zn 2p, Cd 2p and Hg 2p regions of the complexes **1**, **2** and **3**. Zn exhibits +2 oxidation by showing a peak at 1021.96 eV in *Fig.* 6a (complex **1**) corresponds to +2 oxidation state and $L_3M_{45}M_{45}$ Auger transition of Zn atoms shows a peak at 988.0 eV confirming the +2 oxidation state of Zn atoms in the complex as in ZnO.[46] It confirms the oxide coordination of $-NO_2$ group to the Zn atom ($-Zn-O-N-O$) along with IR results. Similarly Cd 3d peak observed at 405.6 eV (*Fig.* 6b) clearly indicates +2 oxidation state for Cd in complex **2**.[47] These results are supportive to our electrochemical observation on these complexes discussed in section 3.4. Hg atoms of the complex 3 exhibits +2 oxidation state by showing a peak at 103.2 eV for Hg $4f_{7/2}$ transition in *Fig.* 6c.[48] Unfortunately we could not confirm the existence of Hg(I) oxidation state as observed in the electrochemical studies of this complex (section 3.4) with XPS. N 1s region of all the three complexes clearly differentiates between –N coordination of pyridine (399.8 eV, BE) and the presence of

'nitrito' nitrogen (404.0 eV, BE).[49] O 1s peak of all the complexes is observed around 533.0 eV and it can be assigned to the oxygen present in 'nitrito' ligand.[50] The valence band region of the XPS for the three complexes clearly indicates the complete hybridization of valance orbitals of metal atoms with N and O atoms (not shown).

APPLICATION OF THE COMPLEXES – IN VITRO BIOLOGICAL SCREENING OF LIGAND AND Zn(II), Cd(II) AND Hg(II) COMPLEXES

Antibacterial Screening

Fig. 9 shows the antibacterial activity of the complexes **1**, **2** and **3** and the free ligand 4AP. Antibacterial activities of the complexes **1**, **2** and **3** are generally better than the free ligand, 4AP for the bacteria *R. planticola* and *S. flexineri*. But the activity against *P. aeruginosa* is not good for the complexes **1**, **2** and **3** compared to the 4AP. It is commonly believed that complexation helps to improve the antibacterial activity due to various properties of the complexes like decreasing polarizability of the metal ion, increasing lipophilic character, etc.[8–10,19,20] But our results suggest that the activity of the complexes **1**, **2** and **3** against *P. aeruginosa* is completely different from the other two though all the three bacteria are classified as 'gram-negative'. Hence more studies are required further to explore this

strange behavior. The complex **2** shows better activity than the other two complexes. It is worth to note here that the complexes **2** and **3** become more active above 50 µg/ml concentration, which is minimum inhibitory concentration (MIC). It is evident in the case of complex **2**, above 50 µg/ml concentration the activity against *R. planticola* increases rapidly than *S. flexineri*. Therefore the activity of the complexes and free ligand follows the order: 2 > 3 > 1 > 4AP against the bacteria *R. planticola* and *S. flexineri*; but the activity is almost similar for the complexes and the free ligand against *P. aeruginosa* particularly at lower concentrations. Above 50 µg/ml concentrations, the complexes **2** and **3** act better against *P. aeruginosa*. Hence the activity is highly dependent on concentration of the complexes.

Antifungal Screening

Results of the fungicidal screening are presented in *Table* 4. The complexes **1**, **2** and **3** show better activities against the fungi, *C. albicans* and *A. niger* compared to the free ligands, 4AP and NO_2^-. The complex **2** shows better antifungal activity than the other complexes. Higher concentrations of the complexes are generally more active, i.e., the antifungal activity of the complexes is also concentration dependent like their antibacterial activity. But the activity of the complexes against the tested fungi, *C.*
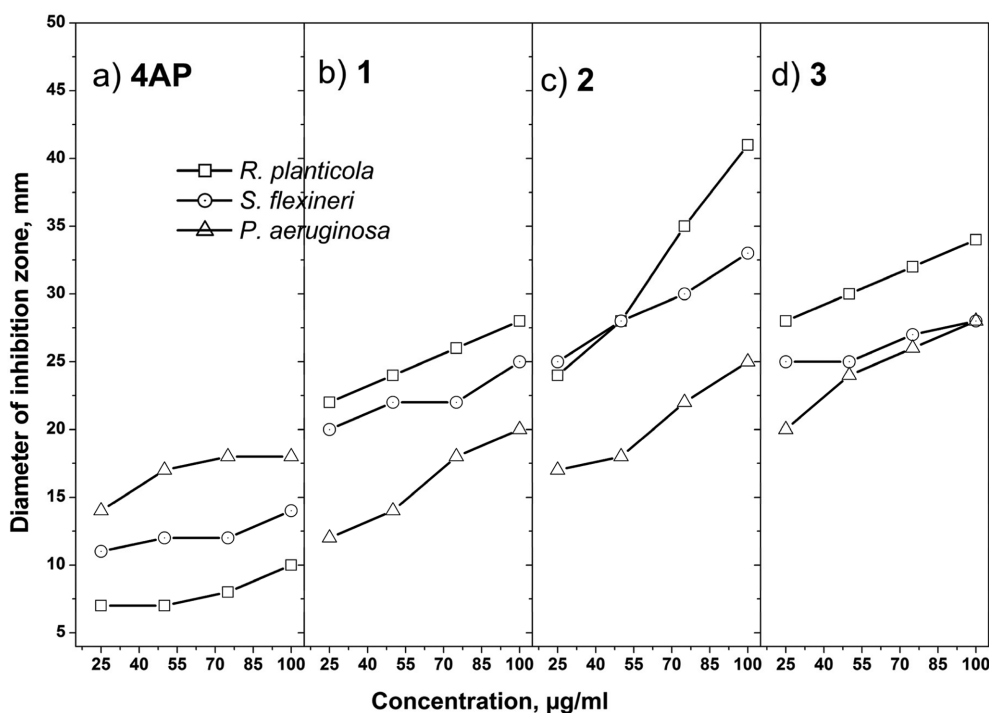
Figure 9. Antibacterial activity of the (a) ligand 4AP and complexes (b) **1**, (c) **2** and (d) **3** against the bacteria, *R. planticola, S. flexineri* and *P. aeruginosa*.

Table **4.** Antifungal activities of compounds and standard reagents

Compound	Fungus tested	Antifungal activity at concentration (μgml^{-1})		
		400	200	100
Ligand(NO$_2^-$)	C.albicans	*	*	*
	A.niger	*	*	*
Ligand(4AP)	A.niger	**	*	*
	C.albicans	**	*	*
Complex **1**	A.niger	***	***	**
	C.albicans	***	***	**
Complex **2**	A.niger	****	****	***
	C.albicans	****	****	***
Complex **3**	A.niger	****	***	***
	C.albicans	****	***	***

*–poor/no activity; **–moderate activity; ***–good activity; ****– excellent activity.

albicans and *A. niger* are similar and there is no difference in activity like their antibacterial performance. The antifungal activity of the complexes follows the same order of their antibacterial activity.

CONCLUSION

4-aminopyridine acts as a neutral monodentate ligand and coordinates through the ring nitrogen. The NO$_2^-$ ligand coordinates to the metal ion through O atom (−O−N=O) which is supported by IR and XPS results. The present study reveals a tetrahedral geometry for Zn(II), Cd(II) and Hg(II) complexes which possesses four coordinated geometry. The results of antibacterial and antifungal activity show that complexes are highly toxic than the free ligands against the tested bacteria and fungi. The antimicrobial activity of the complexes is concentration dependent. The Cd(II) complex shows better antibacterial and antifungal activity than the other two complexes. A need for the refinement on the theory on the activity of the complexes against microorganisms can be envisaged from our antibacterial studies.

REFERENCES

1. Nagar, R. *J. Inorg. Biochem.* **1990**, *40*, 349.
2. Cavagiolio, G.; Benedetto, L.; Boccaleri, E.; Colangelo. D.; Viano, I.; Osella, D. *Inorg. Chim. Acta* **2000**, *305*, 61.
3. Teiichi, Y. *Am. J. Physiol.* **1995**, *269*, 556.
4. Murrow, B. W. *J. Physiol. Lond.* **1994**, *480*, 247.
5. Jin, S.; Fredholm, B. B. *Neuropharmacology* **1994**, *33*, 1039.
6. Chelucci, G. *Coord. Chem. Reviews* **2013** DOI: 10.1016/j.ccr.2012.12.002.
7. Sorensen, J. R. J.; Sigel, H. *Met. Ions. Biol. Syst.* **1982**, *14*, 77.
8. Al-Amiery, A. A; Kadhum, A. A. H.; Mohamad, A. B. *Bioinorg. Chem. Appl.* **2012**, DOI: 10.1155/2012/795812.
9. Thangadurai, T. D.; Natarajan, K. *Transition Met. Chem.* **2001**, *26*, 500.
10. Tweedy, B. G. *Phytopathology* **1964**, *55*, 910.
11. Nakamoto, K. *Infared and Raman Spectra of Inorganic and Coordination Compounds*, Part B, 5th ed.; John Wiley and sons: New York, 1997.
12. Ostrowski, A. D.; Ford, P. C. *Dalton Trans.* **2009**, 10660.
13. Kinali-Demirci, S.; Demirci, S.; Kurt, M. *Spectrochim. Acta, Part A* **2013**, *106*, 12.
14. Sultana, N.; Naz, A.; Arayne, M. S.; Mesaik, M. A. *J. Mol. Struct.* **2010**, *969*, 17.
15. Chandra, S.; Gupta, L. K. *Spectrochim. Acta, Part A* **2004**, *60*, 1751.
16. Deshayes, S.; Liagre, M.; Loupy, A.; Luche., J. L.; Petit., A. *Tetrahedron* **1999**, *55*, 10851.
17. Singh, V.; Kumar, P.; Sanghi, R. *Prog. Polym. Sci.* **2012**, *37*, 340.
18. Bogdal, D.; Pielichowski, J.; Penczek, P.; Prociak, A. *Adv. Polym. Sci.* **2003**, *163*, 51.
19. Celenk, E.; Kantekin, H. *Dyes Pigments* **2009**, *80*, 93.
20. Singh, R. V.; Chaudhary, P.; Chauhan, S.; Swami, M.; *Spectrochim. Acta, Part A* **2009**, *72*, 260.
21. Raman, N.; Kulandaisamy, A.; Thangaraja, C.; Jeyasubramainan, K. *Trans. Met. Chem.* **2003**, *28*, 2.
22. Chaudhary, A.; Singh, R. V. *Phosphorus, Sulphur Silicon Relat. Elem.* **2003**, *178*, 603.
23. Kelkar, V. D.; Kanase, D. G.; Kadam, S. S.; Takale, S. T. *Asian J. Chem.* **2007**, *19*, 3599.
24. Ochoa, J. B.; Udekwu, A. O.; Billar, T. R.; Curran, R. D.; Cerra, F. B.; Simmons, R. L.; Pietzman, A. B. *Ann. Surg.* **1991**, *214*, 621.
25. Arnaudov, M. G.; Ivanova, B. B.; Dinkov, Sh. *Vibr. Spectrosc.* **2005**, *37*, 145.
26. Arnaudov, M. G.; Ivanova, B. B.; Dinkov, Sh. *Cents. Eur. J. Chem.* **2004**, *2*, 589.
27. Bakiler, M.; Maslov, I. V.; Akyuz, S. *J. Mol. Struct.* **1999**, *475*, 83.
28. Akyuz, S.; Dempster, A. B.; Morehouse, R. L.; Suzuki, S. *J. Mol. Struct.* **1973**, *17*, 105.
29. Chattapadhyay, T.; Ghosh, M.; Majee, A.; Nethaji, M.; Das,

D. *Polyhedron* **2005**, *24*, 1677.
30. Basolo, F.; Hammaker, G. S. *J. Am. Chem. Soc.* **1960**, *82*, 1001.
31. Nakamoto, K.; Fujita, J.; Murata, H. *J. Am. Chem. Soc.* **1958**, *80*, 4817.
32. Penland, R. B.; Lane, T. J.; Quagliano, J. V. *J. Am. Chem. Soc.* **1956**, *78*, 887.
33. Basolo, F.; Hammaker, G. S. *Inorg. Chem.* **1962**, *1*, 1.
34. Nakamoto, K. *Infrared Spectra of Inorganic and Coordination Compounds*; John Wiley & Sons: New York, 1963.
35. Blyholder, G.; Kittila, A. *J. Phys. Chem.* **1963**, *67*, 2147.
36. Silverstein, R. M.; Bassler, G. C.; Morrill, T. C. *Spectrometric Identification of Organic Compounds*, 5th ed., Wiley: New York, 1991.
37. Rajasekar, K.; Ramachandramoorthy, T.; Balasubramaniyan, S. *Res. J. Chem. Sci.* **2013**, *3*(3), 48.
38. Choi, J.-H.; Oh, I.-G.; Lim, W.-T.; Ryoo, K. S.; Kim, D. I.; Park, Y. C. *J. Korean Chem. Soc.* **2005**, *49*, 239.
39. Cleare, M. J.; Griffith, W. P. *J. Chem. Soc. A* **1967**, 1144.
40. Machura, B. *Polyhedron* **2004**, *23*, 2363.
41. Hatzidumitrious, A.; Bolos, C. A. *Polyhedron* **1998**, *17*, 1779.
42. Melnik, M.; Gyoryova, K.; Skorsepa, J.; Holloway, C. E. *J. Coord. Chem.* **1995**, *35*, 179.
43. Kharisov, B. I.; Blanco-Jerez, L. M.; Garcia-Luna, A. *Rev. Soc. Quim. Mex.* **1999**, *43*, 51.
44. Rajavel, R.; Senthilvedivu, M.; Anitha, C. *E-Journal of Chemistry* **2008**, *5*, 620.
45. Materazzi, S.; Vasca, E. *Thermochim. Acta* **2001**, *373*, 11.
46. Barba, A.; Clausell, C.; Jarque J. C.; Monz M. *J. Eur. Ceram. Soc.* **2011**, *31*, 2119.
47. Iwai, H.; Umeki, T.; Yokomatsu, M.; Egawa, C. *Surf. Sci.* **2008**, *602*, 2541.
48. Bai, X.; Jie, W.; Zha, G.; Zhang, W.; Li, P.; Hua, H.; Fu, L. *Appl. Surf. Sci.* **2009**, *255*, 7966.
49. Guo, Y.; Yan, N.; Yang, S.; Liu, P.; Wang, J.; Qu, Z.; Jia, J. *J. Hazard. Mater.* **2013**, DOI: 10.1016/j.jhazmat.2012.01.048.
50. Jenniskens, H. G.; van Essenberg, W.; Kadodwala, M.; Kleyn, A. W. *Surf. Sci.* **1998**, 402–404, 140.